

## The W40 Cloud Complex

Steven A. Rodney

*Institute for Astronomy, University of Hawaii*  
 2680 Woodlawn Dr., Honolulu, HI 96822, USA

Bo Reipurth

*Institute for Astronomy, University of Hawaii*  
 640 N. Aohoku Place, Hilo, HI 96720, USA

**Abstract.** The W40 complex is a nearby site of recent massive star formation composed of a dense molecular cloud adjacent to an HII region that contains an embedded OB star cluster. The HII region is beginning to blister out and break free from its envelope of molecular gas, but our line of sight to the central stars is largely obscured by intervening dust. Several bright OB stars in W40 - visible at optical, infrared, or cm wavelengths - are providing the ionizing flux that heats the HII region. The known stellar component of W40 is dominated by a small number of partly or fully embedded OB stars which have been studied at various wavelengths, but the lower mass stellar population remains largely unexamined. Despite its modest optical appearance, at 600 pc W40 is one of the nearest massive star forming regions, and with a UV flux of about 1/10th of the Orion Nebula Cluster, this neglected region deserves detailed investigation.

### 1. Overview

The star forming region known as W40 consists of three interrelated components. First, there is the cold molecular cloud, which is designated using Galactic coordinates as G28.8+3.5, following Goss & Shaver (1970). This dark cloud has an angular extent on the order of one degree, and is centered around a dense molecular core with a diameter of approximately  $20'$ , identified as TGU 279-P7 in the recent extinction atlas of Dobashi et al. (2005).

Adjacent to this molecular cloud is the large blister HII region denoted as W40 (Westerhout 1958), and also labeled as S64 by Sharpless (1959), as RCW 174 by Rodgers, Campbell, & Whiteoak (1960), or LBN 90 in the Lynds (1965) catalog of bright nebulae. The W40 HII region is centered on J2000 coordinates  $18^h31^m29^s$ ,  $-2^\circ05'4''$ , and has a diameter of  $\sim 6'$ . The space between the hot, ionized HII region and the cold molecular cloud is marked by a thin CII region and an accompanying neutral interface (Vallée 1987).

Lastly, the W40 region hosts an embedded stellar cluster that is dominated by three bright IR sources (Zeilik & Lada 1978). These bright OB stars are the primary excitation sources for the W40 HII region (Smith et al. 1985) and show evidence for substantial circumstellar envelopes (Vallée & MacLeod 1994). The W40 cluster is heavily obscured along our line of sight by the surrounding molecular cloud, which provides  $A_V \sim 10$  magnitudes of visual extinction throughout, and as much as  $A_V = 17$  mag at

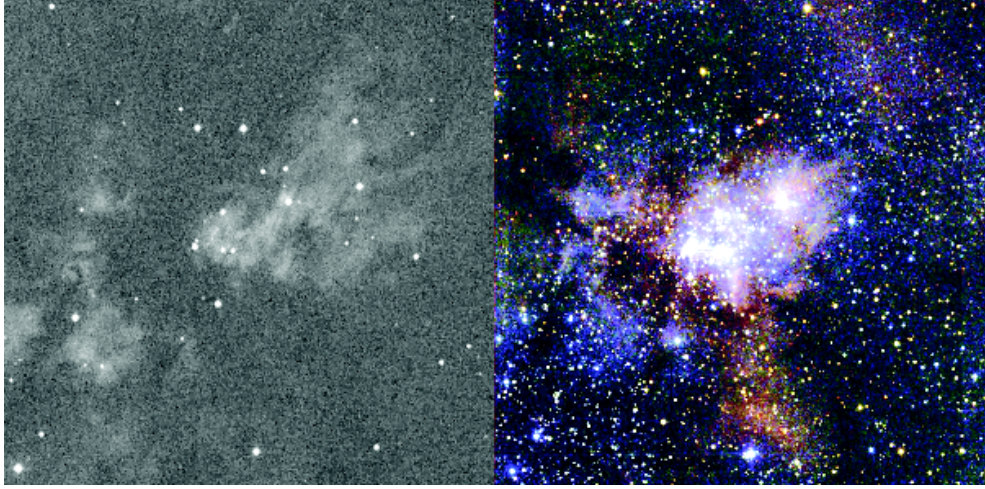


Figure 1. The W40 region seen on (left) the red Digitized Sky Survey and (right) at JHK with 2MASS. The field is approximately  $17 \times 17$  arcmin, corresponding to a little less than 3 pc on the side at 600 pc. North is up and east is left. Courtesy K. Getman.

the dense center (Reyl   & Robin 2002). Figure 1 shows the W40 region in the optical from the Digitized Sky Survey and in the infrared from the 2MASS survey.

## 2. Distance

The distance to W40 has not yet been determined to any satisfactory precision. Measurements of the  $H109\alpha$  atomic recombination line at  $0.7 \text{ km s}^{-1}$  (Reifenstein et al. 1970), the  $\lambda 18 \text{ cm}$  OH absorption line at  $6.3 \text{ km s}^{-1}$  (Downes 1970) and the  $21 \text{ cm}$  HI absorption line along the line of sight at  $7.2 \text{ km s}^{-1}$  (Radhakrishnan et al. 1972) collectively suggest a rough kinematic distance estimate of 300-900 pc based on the assumption that the cloud is in circular motion about the Galactic center. Estimates based on the radio/IR continuum of W40's stellar component allow for a similar range from 400 pc (Crutcher & Chu 1982) to 700 pc (Smith et al. 1985). Using OH line measurements with a unique distance determination technique, Kolesnik & Iurevich (1983) calculated a distance of 600 pc.

Adopting a conservative mean of 600 pc places W40 at a distance of 37 pc above the Galactic plane. The dense central region of the molecular cloud is then  $\sim 3.5$  pc in diameter, and the width of the HII region measures  $\sim 1$  pc.

## 3. The HII Region and Molecular Cloud

After the initial discoveries of the W40 radio emission nebula and its associated HII region around 1960, subsequent radio detections were recorded over a wide range of frequencies. By the early 1970s the radio spectrum was well-constrained from 408 MHz to 5 GHz. Table 1 summarizes the radio observations of the HII region's free-free continuum and carbon recombination lines in the CII shell. The median flux density

Table 1. Radio Observations

Freq. (GHz)	Wave. (cm)	Flux <sup>a</sup> (Jy)	Telescope Location <sup>b</sup>	HPBW (arc min)	Reference
Continuum Observations					
0.328	91.5	34	VLA-C - 3.4 km	46''	Vallée & MacLeod (1991)
0.408	73.5	34	Molonglo - 1.6 km	1.4 × 2.5	Kesteven (1968)
0.408	73.5	25	Molonglo - 1.6 km	2.6 × 3.4	Shaver & Goss (1970)
0.610	49.2	35	Jodrell Bank - 76 m	30	Moran (1965)
0.960	31.3	25	Owens Valley - 27 m	48	Wilson (1963)
1.390	21.6	50	Dwingeloo - 25 m	34.2	Westerhout (1958)
1.400	21.4	33	Green Bank - 91 m	10	Felli & Churchwell (1972)
1.414	21.2	36	Green Bank - 91 m	10	Altenhoff et al. (1970)
1.465	20.5	30	VLA-C - 3.4 km	12''	Vallée & MacLeod (1991)
2.695	11.1	34	Green Bank - 43 m	11	Altenhoff et al. (1970)
4.86	6.17	-	VLA-B - 10.6 km	~ 2''	Molinari et al. (1998)
5.000	6.00	35	Fort Davis - 26 m	11	Altenhoff et al. (1970)
5.000	6.00	32	Parkes - 64 m	4.0	Goss & Shaver (1970)
5.009	5.99	35	Green Bank - 43 m	6.5	Reifenstein et al. (1970)
14.94	2.0	-	VLA-B - 10.6 km	~ 2''	Molinari et al. (1998)
C100 $\alpha$ / C125 $\alpha$ Observations					
(GHz)	(cm)	(mJy)		(arc min)	
1.425	21.0	84 <sup>c</sup>	Effelsberg - 100 m	8.5	Pankonin et al. (1977)
3.327	9.01	156	Algonquin - 46 m	8.2	Vallée (1987)
6.482	4.62	86	Algonquin - 46 m	4.3	Vallée (1987)

<sup>a</sup> Value quoted is the integrated flux density of the HII region continuum<sup>b</sup> Single dish diameter in meters; longest interferometer baseline in km<sup>c</sup> Deduced from their values of brightness temperature and angular size (Vallée 1987)

NOTE — Adapted from Table 1 of Vallée (1987)

Table 2. Millimeter Observations

Molecular Transition	Wave (mm)	Telescope Location	HPBW (arc sec)	Reference
HCO <sup>+</sup> J=1-0	3.36	Crimean Astr.Obs. - 22 m	40	Pirogov et al. (1995)
C <sup>18</sup> O J=1-0	2.73	Pico Veleta - 30 m	22	Vallée et al. (1992)
<sup>13</sup> CO J=1-0	2.72	Pico Veleta - 30 m	22	Vallée et al. (1992)
<sup>12</sup> CO J=1-0	2.6	Kitt Peak - 11 m	1.2	Wilson et al. (1974)
<sup>12</sup> CO J=1-0	2.6	McDonald Obs. - 5 m	2.3	Zeilik & Lada (1978)
<sup>12</sup> CO J=1-0	2.6	Holmdel - 7 m	1.7	Blitz et al. (1982)
<sup>12</sup> CO J=1-0	2.6	Purple Mountain - 13.7 m	50	Zhu et al. (2006)
<sup>13</sup> CO J=2-1	1.36	Pico Veleta - 30 m	12	Vallée et al. (1992)
<sup>13</sup> CO J=2-1	1.36	KOSMA - 3 m	120	Zhu et al. (2006)
C <sup>18</sup> O J=2-1	1.37	Kitt Peak - 12 m	32	Vallée et al. (1992)
<sup>13</sup> CO J=2-1	1.36	Kitt Peak - 12 m	32	Vallée et al. (1992)
<sup>13</sup> CO J=3-2	0.9	KOSMA - 3 m	80	Zhu et al. (2006)
<sup>12</sup> CO J=3-2	0.87	KOSMA - 3 m	80	Zhu et al. (2006)

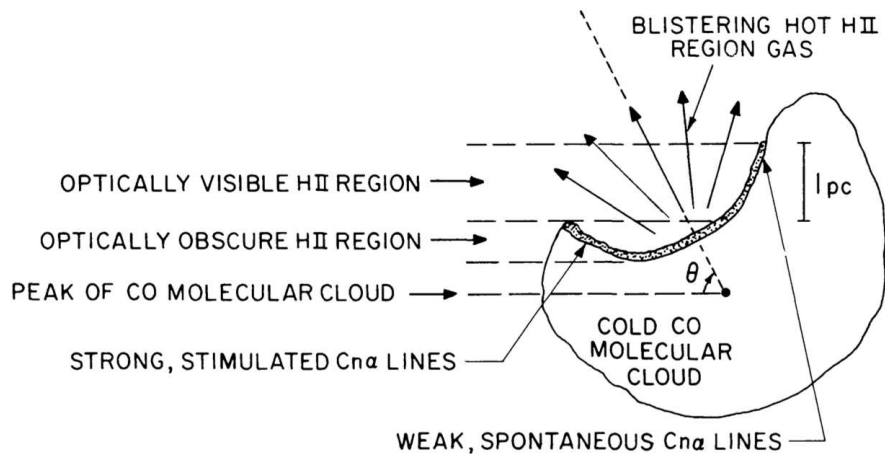


Figure 2. Sketch of the relative positioning of the warm CII region ( $\sim 10^2$  K) between the hot blister HII region ( $\sim 10^4$  K) to the north and the cold CO molecular cloud ( $\sim 10$  K) to the south. Taken from Vallée (1987)

of the radio continuum in the HII region is 34 Jy. The most detailed radio continuum analysis to date is from the VLA observations of Vallée & MacLeod (1991), which show a linear increase in the flux density across the HII region from the surrounding interstellar medium in the NE to the molecular cloud edge in the SW. Their maps also suggest the presence of a  $1.7'$  shell around the star IRS2a.

The TGU 279 molecular cloud has also been extensively mapped at millimeter wavelengths. These observations are summarized in Table 1. The properties of the molecular cloud derived from these observations are strongly model-dependent. Vallée et al. (1992) find that the total mass of the central cloud core out to a radius of 0.4 pc is  $\sim 100M_{\odot}$ , and the density profile goes as  $r^{-1}$ . Zhu, Wu, & Wei (2006) measured the mass of the cloud core at the center of the outflow to be 188 or 319  $M_{\odot}$ , depending on the transition used for the estimate. The larger cloud complex probably has a mass of order  $10^4 M_{\odot}$ . Additionally, the magnetic field strength within W40 has been determined from Zeeman measurements of the 1665 and 1667 MHz OH lines to be  $B = -14.0 \pm 2.6 \mu\text{G}$  (Crutcher et al. 1987).

The first detailed infrared examination of the W40 region was carried out by Zeilik & Lada (1978). These authors find that the carbon recombination lines and CO molecular lines have velocities that are offset from the published hydrogen recombination lines by  $\sim 4 \text{ km s}^{-1}$ . In addition, the bright IR sources are spatially displaced from the CO peak, suggestive of a blister HII region expanding away from the dense molecular cloud core.

In 1982, Crutcher & Chu built on this conclusion by reviewing the available radio recombination line measurements, supplemented with their own molecular and H $\alpha$  maps. These authors note the presence of two molecular components with velocities that differ by about  $3 \text{ km s}^{-1}$ , and suggest that they correspond to the compressed gas on either side of the HII region, along our line of sight.

Vallée (1987) took measurements of Cn $\alpha$  recombination lines in the warm neutral interface between the hot HII region and the cold molecular cloud. Fitting a model to

Table 3. Stellar Sources in the W40 Cluster

ID: W40-	R.A. (2000)	Dec. (2000)	References
VLA 1	18 <sup>h</sup> 31 <sup>m</sup> 14 <sup>s</sup> .8	-02°03'50''	4
VLA 2	18 31 15.3	-02 04 15	4
IRS 2b OS 2b	18 31 22.3	-02 05 32	2
VLA 3	18 31 22.3	-02 06 19	4
VLA 4	18 31 23.2	-02 06 18	4
VLA 5	18 31 23.6	-02 05 35	4
VLA 6	18 31 23.6	-02 05 28	4
IRS 3a OS 3a	18 31 24.0	-02 04 11	1, 2, 3
VLA 7 IRS 2a OS 2a	18 31 24.0	-02 05 30	1, 2, 3, 4
OS 2c	18 31 25.2	-02 05 10	2
VLA 8 IRS 1c	18 31 26.0	-02 05 17	2, 4
OS 4a	18 31 26.5	-02 04 31	2
VLA 9	18 31 27.3	-02 05 04	4
VLA 10	18 31 27.5	-02 05 12	4
VLA 11	18 31 27.6	-02 05 18	4
VLA 12	18 31 27.6	-02 05 13	4
VLA 13 IRS 1d OS 1d	18 31 27.7	-02 05 10	2, 4
VLA 14	18 31 27.7	-02 05 20	4
VLA 15 IRS 1a OS 1a	18 31 27.8	-02 05 22	1, 2, 3, 4
VLA 16	18 31 28.0	-02 05 18	4
VLA 17	18 31 28.6	-02 05 29	4
VLA 18 IRS 1b	18 31 28.7	-02 05 30	2, 4
VLA 19	18 31 28.7	-02 05 22	4
VLA 20	18 31 30.2	-02 07 18	4

REFERENCES — (1) Zeilik & Lada (1978), (2) Smith et al. (1985),  
 (3) Vallée & MacLeod (1991), (4) Rodríguez, Rodney, & Reipurth (2008, in preparation)

their observations, they were able to constrain the properties of the thin CII shell and surmise that the stimulated Cn $\alpha$  line emission must be driven by a high background temperature provided by the partially obscured HII region.

With these observations we may begin to draw a coherent picture of the history and current state of the W40 molecular cloud complex. Star formation in this region was initiated perhaps several million years ago by an external shock which caused a compression of the molecular gas and a distinct shift in the velocity of some of the molecular hydrogen. The subsequent formation of a number of O and B stars created the HII region, with a center offset by  $\sim 2'$  to the northeast of the molecular cloud core. This HII region began to expand and ionize the surrounding gas, eventually breaking through to reveal some patchy H $\alpha$  emission. A screen of molecular hydrogen and dust still remains along our line of sight, obscuring most of the embedded HII region, and the thin shell between these cold and hot media is dominated by stimulated Cn $\alpha$  emission. A schematic representation of this geometry, taken from Vallée (1987), is shown in Figure 2.

#### 4. The Stellar Sources

In contrast to the relatively detailed investigations of the cloud complex, very little work has been done on the underlying stellar population. Three dominant IR sources in W40 were noted by Zeilik & Lada (1978), and subsequent observations revealed that six of the seven brightest IR sources can be matched with optical counterparts (Smith et al. 1985). Recent high-resolution radio continuum observations using the VLA telescope have produced detailed maps of the W40 cluster at 3.6 cm (Rodríguez, Rodney, & Reipurth 2008, in preparation). These measurements reveal that the W40 cluster harbors 20 compact radio sources, 15 of which have IR counterparts, and 10 of which show substantial variability in their radio flux. Figure 3 shows a  $\sim 30''$  band of 11 of these VLA sources. The brightest of W40's optical, IR and radio sources are catalogued in Table 3. The entire W40 cluster is shown in Figure 4, which presents a composite JHK' image of the W40 cluster taken with the University of Hawaii 2.2m telescope.

The high energy emission of the stars in the W40 cluster is now being examined with an X-ray study using the Chandra space telescope (Getman, K. et al. 2008, in preparation). Figure 5 shows a preliminary Chandra X-ray map of the cluster, which reveals scores of X-ray point sources coincident with the optical and IR stellar cluster. Some diffuse X-ray emission at the cluster center has also been detected.

The infrared spectral energy distributions of the brightest cluster members were examined by Smith et al. (1985), and later millimeter observations of these sources with the James Clerk Maxwell Telescope in Hawaii have revealed further evidence for substantial circumstellar material surrounding IRS1a and IRS2a (Vallée & MacLeod 1994). Smith et al. (1985) have shown that the circumstellar material around these sources is not an important source of IR re-radiation in W40, but rather the diffuse dust throughout the region is the dominant absorbing medium. Molecular absorption lines towards IRS 1a, the brightest of the IR sources,<sup>1</sup> have been used to deduce column densities, temperatures, and abundance ratios in the foreground region of the W40 molecular cloud (Shuping et al. 1999).

The Midcourse Space Experiment (MSX) satellite has observed the W40 region, and a map obtained at  $8\ \mu\text{m}$  is shown in Figure 6. Here the full structure of the W40 region is seen with minimal interference from obscuring dust clouds. We see that W40 consists of two interconnected cavities, forming an hour-glass shape. The main cluster is located just northwest of the narrow waist where the two cavities are joined. The total extent of the two cavities is roughly  $17 \times 28$  arcmin, which at the assumed distance of 600 pc translates into about  $3 \times 5$  pc. Numerous point sources are detected by MSX in W40, but only one has a good match with the coordinates of the sources listed in Table 3: the MSX source G028.7799+03.4978 is  $2.5''$  from IRS 2a. For this source, MSX measured flux densities of 27.1, 41.7, 55.7 and 78.8 Jy at 8, 12, 15 and  $21\ \mu\text{m}$ , respectively.

Zhu, Wu, & Wei (2006) obtained  $^{12}\text{CO}$  J=3-2 and  $^{13}\text{CO}$  J=2-1 and J=3-2 observations of the W40 region and found a molecular outflow associated with the molecular cloud on the southwestern rim of the HII region. The spatial position of the outflow

---

<sup>1</sup>Although IRS1a is the brightest IR source in the region, Smith et al. (1985) present evidence that it is not the most luminous. The more heavily obscured IRS2a is considered to be the more luminous object, and it appears to be the primary source of ionizing radiation.

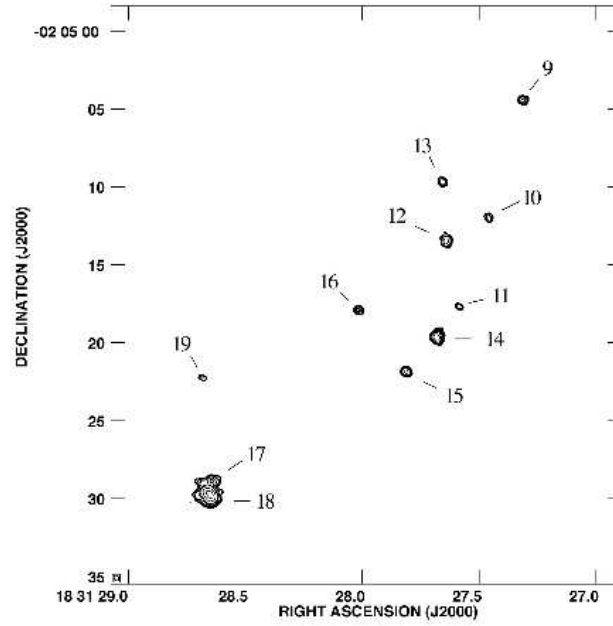


Figure 3. VLA contour map showing the central cluster of compact radio sources in the W40 region. The labels correspond to the ID numbers indicated in Table 3. The majority of these sources show variability on timescales of  $< 20$  days. From Rodríguez, Rodney, & Reipurth (2008, in preparation).

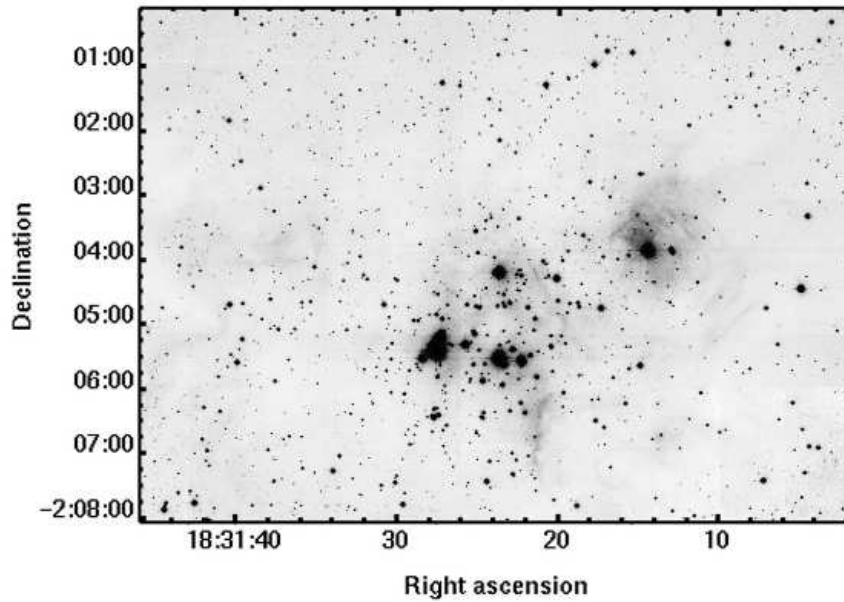


Figure 4. Composite JHK' image showing the W40 region at  $\sim 2 \mu\text{m}$ . The three brightest infrared sources have been identified as OB stars powering the HII region. Coordinates are J2000. From Rodríguez, Rodney, & Reipurth (2008, in preparation).

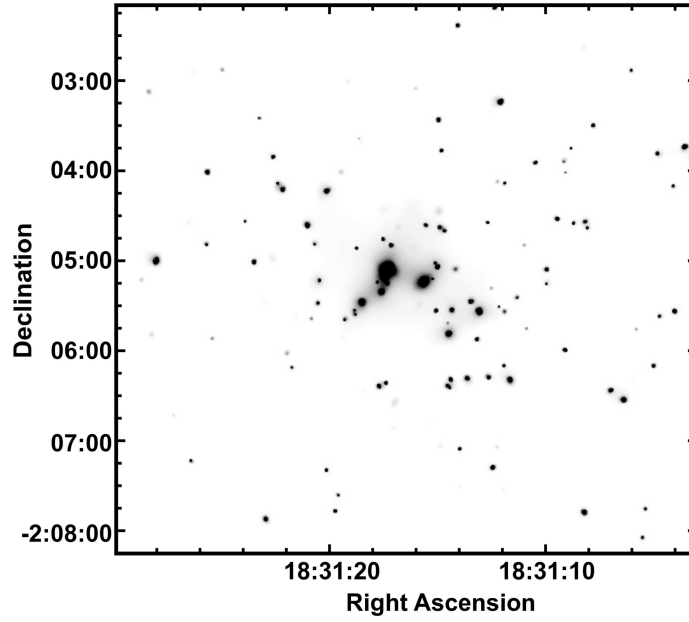


Figure 5. Close-up adaptively smoothed Chandra view of the  $6.5' \times 6'$  field around the ionizing OB stars. Smoothing has been performed in the (0.5-8.0) keV band at the 2.5 sigma level, and gray scales are logarithmic. Over 100 X-ray point sources along with the diffuse X-ray emission can be seen. Coordinates, given as J2000, are only approximate. Courtesy K. Getman.

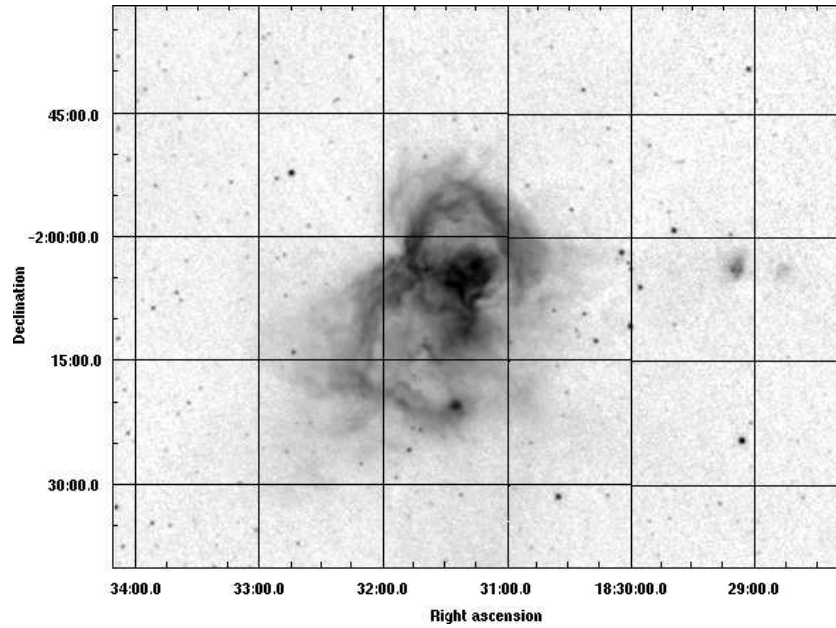


Figure 6. The W40 region as seen by MSX at a wavelength of  $8 \mu\text{m}$ . The HII region is here seen with minimal impact of extinction, and appears as an hour-glass shaped structure about  $3 \times 5$  pc in extent.



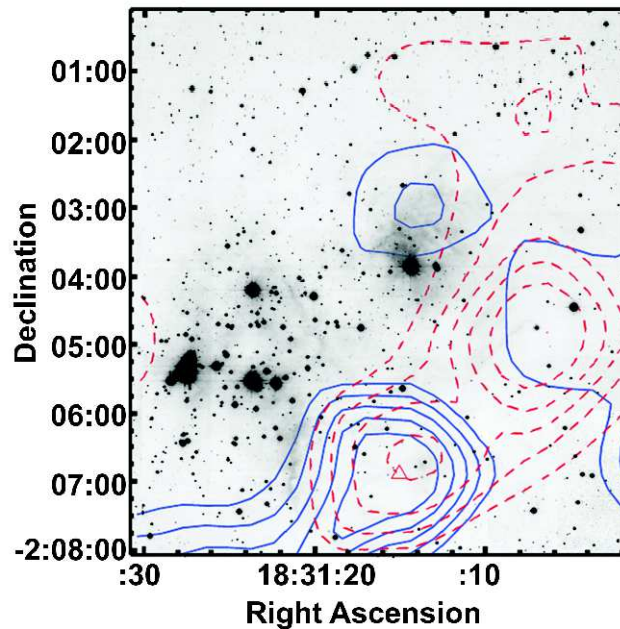


Figure 7. The molecular cloud to the southwest of the W40 cluster contains a weak molecular outflow discovered by Zhu et al. (2006). The solid line is the blue lobe, and the dotted line is the red lobe. A second outflow is possibly present farther to the north. The millimeter observations are superposed on the  $2\ \mu\text{m}$  image from Figure 4.

relative to the cluster is seen in Figure 7. Neither the MSX nor the IRAS catalogues show a source at the center of the outflow, suggesting that a very young, very embedded source is powering the outflow activity. Clearly star formation is still taking place in the W40 region.

**Acknowledgements.** We are thankful to Konstantin Getman for providing Figures 1 and 5 and for a thorough and very helpful referee's report. This work has made use of The Digitized Sky Surveys, produced at the Space Telescope Science Institute. The images of these surveys are based on photographic data obtained using the Oschin Schmidt Telescope on Palomar Mountain and the UK Schmidt Telescope. This research has made use of NASA's Astrophysics Data System; data products from the Two Micron All Sky Survey, which is a joint project of the University of Massachusetts and the Infrared Processing and Analysis Center/California Institute of Technology, funded by the National Aeronautics and Space Administration and the National Science Foundation; images from the MidCourse Space Experiment; and the SIMBAD database, operated at CDS, Strasbourg, France. BR was supported in part by the NASA Astrobiology Institute under Cooperative Agreement No. NNA04CC08A and by the NSF through grants AST-0507784 and AST-0407005.

## References

- Altenhoff, W. J., Downes, D., Goad, L., Maxwell, A., & Rinehart, R. 1970, *A&AS*, 1, 319
- Blitz, L., Fich, M., & Stark, A. A. 1982, *ApJS*, 49, 183
- Crutcher, R. M. & Chu, Y. H. 1982, in *ASSL Vol. 93: Regions of Recent Star Formation*, eds. R.S. Roger & P.E. Dewdney, 53
- Crutcher, R. M., Troland, T. H., & Kazes, I. 1987, *A&A*, 181, 119
- Dobashi, K., Uehara, H., Kandori, R., Sakurai, T., Kaiden, M., Umemoto, T., & Sato, F. 2005, *PASJ*, 57, SP1, 1
- Downes, D. 1970, *Astrophys. Lett.*, 5, 53
- Felli, M. & Churchwell, E. 1972, *A&AS*, 5, 369
- Goss, W. M. & Shaver, P. A. 1970, *Australian Journal of Physics Astrophysical Supplement*, 14, 1
- Gutermuth, R. A., Bourke, T. L., Allen, L. E., Myers, P. C., Megeath, S. T., et al. 2008, *ApJ*, 673, 151
- Kesteven, M. J. L. 1968, *Australian Journal of Physics*, 21, 369
- Kolesnik, I. G. & Iurevich, L. V. 1983, *Astrofizika*, 19, 761
- Lynds, B. T. 1965, *ApJS*, 12, 163
- Molinari, S., Brand, J., Cesaroni, R., Palla, F., & Palumbo, G. G. C. 1998, *A&A*, 336, 339
- Moran, M. 1965, *MNRAS*, 129, 447
- Pankonin, V., Barsuhn, J., & Thomasson, P. 1977, *A&A*, 54, 335
- Pirogov, L., Zinchenko, I., Lapinov, A., Myshenko, V., & Shul'Ga, V. 1995, *A&AS*, 109, 333
- Radhakrishnan, V., Goss, W. M., Murray, J. D., & Brooks, J. W. 1972, *ApJS*, 24, 49
- Reifenstein, E. C., Wilson, T. L., Burke, B. F., Mezger, P. G., & Altenhoff, W. J. 1970, *A&A*, 4, 357
- Reyl , C. & Robin, A. C. 2002, *A&A*, 384, 403
- Rodgers, A.W., Campbell, C.T., & Whiteoak, J.B. 1960, *MNRAS*, 121, 103
- Sharpless, S. 1959, *ApJS*, 4, 257
- Shaver, P. A. & Goss, W. M. 1970, *Australian Journal of Physics Astrophysical Supplement*, 14, 77
- Shuping, R. Y., Snow, T. P., Crutcher, R., & Lutz, B. L. 1999, *ApJ*, 520, 149
- Smith, J., Bentley, A., Castelaz, M., Gehr , R. D., Grasdalen, G. L., & Hackwell, J. A. 1985, *ApJ*, 291, 571
- Vall e, J. P. 1987, *A&A*, 178, 237
- Vall e, J. P., Guilleaudeau, S., & MacLeod, J. M. 1992, *A&A*, 266, 520
- Vall e, J. P. & MacLeod, J. M. 1991, *A&A*, 250, 143
- . 1994, *AJ*, 108, 998
- Westerhout, G. 1958, *Bull. Astron. Inst. Netherlands*, 14, 215
- Wilson, R. W. 1963, *AJ*, 68, 181
- Wilson, W. J., Schwartz, P. R., Epstein, E. E., Johnson, W. A., Etcheverry, R. D., Mori, T. T., Berry, G. G., & Dyson, H. B. 1974, *ApJ*, 191, 357
- Zeilik, M. & Lada, C. J. 1978, *ApJ*, 222, 896
- Zhu, L., Wu, Y.-F., & Wei, Y. 2006, *Chin. J. Astron. Astrophys.*, 6, 61